

## 2D Exchange NMR Investigation of the $\alpha$ -Relaxation in Poly(ethyl methacrylate) as Compared to Poly(methyl methacrylate)

S. C. Kuebler,<sup>†</sup> D. J. Schaefer,<sup>†</sup> C. Boeffel, U. Pawelzik, and H. W. Spiess\*

Max-Planck-Institut für Polymerforschung, Postfach 3148, D-55021 Mainz, Germany

Received June 16, 1997; Revised Manuscript Received August 14, 1997<sup>®</sup>

**ABSTRACT:** The main chain dynamics of amorphous poly(ethyl methacrylate) (PEMA) and poly(methyl methacrylate) (PMMA) below and above their respective glass transition temperatures  $T_g$  are analyzed by two-dimensional solid-state exchange  $^2\text{H}$  NMR spectroscopy. In both polymers, a restricted mobility of the polymer backbone is already present in the glassy state, as is directly demonstrated and quantified using samples deuterated at the methyl and methylene moieties of the polymer main chain. The unusual main chain mobility below  $T_g$  is coupled to the  $\beta$ -relaxation process, which involves  $180^\circ$  flips of the carboxyl side groups. At their respective glass transition temperatures, the coupling of the  $\beta$ -process to the main chain motions manifests itself differently in both polymers; the smaller ester side group reorients comparatively fast in PMMA, whereas in PEMA, the reorientation of the bulkier side group remains anisotropic and the correlation times are slower by about 1 order of magnitude. Therefore, in PMMA, the  $\beta$ -relaxation predominantly influences the time scale of the  $\alpha$ -relaxation, leading to a particularly high mobility of the main chain itself. In contrast, in PEMA, a slow uniaxial diffusion of the main chain around its local axis sets in at  $T_g$ , the  $\beta$ -process thus affecting mainly the geometry of backbone motions, as is further corroborated by comparing one-dimensional  $^{13}\text{C}$  NMR spectra with two-dimensional exchange  $^2\text{H}$  NMR spectra at higher temperatures. In summary, the coupling of the  $\alpha$ - and  $\beta$ -processes leads to longer mean correlation times for the  $\alpha$ -relaxation in PEMA than in PMMA.

### I. Introduction

In amorphous polymers, the  $\alpha$ -relaxation is linked to the cooperative dynamics of main chain segments in the viscoelastic state, with backbone motions being frozen in at the glass transition temperature  $T_g$ .<sup>1</sup> In contrast, local dynamics of molecular segments, e.g.,  $\beta$ - and  $\gamma$ -relaxations, often involving side group motions, are also pertinent in the glassy state. Recently, in acrylate polymers the molecular nature of the  $\beta$ -relaxation, which is attributed to the rotation of the ester side group, has been investigated in poly(methyl methacrylate) (PMMA)<sup>2</sup> and poly(ethyl methacrylate) (PEMA)<sup>3</sup> by multidimensional solid-state NMR techniques,<sup>4</sup> which provide unique capabilities to access directly the geometry of motion of a particular segment for rotational correlation times ranging from milliseconds to seconds, as are often relevant in polymer dynamics.

In particular, exploiting the chemical shift anisotropy of the carboxyl carbon in two-dimensional (2D) exchange  $^{13}\text{C}$  NMR experiments of PMMA below  $T_g$ , the  $\beta$ -process was determined to consist of a  $180 \pm 10^\circ$  flip of the ester unit accompanied by a restricted main chain rearrangement with a  $\pm 20^\circ$  rms amplitude. Additionally, on the time scale of the  $\beta$ -process, the dynamics was shown to be bimodal, with 50% of the side groups being mobile and the rest only fluctuating around their equilibrium positions. These results were corroborated by 2D exchange  $^2\text{H}$  NMR experiments of the methoxy side group in PMMA, and similar results were obtained from 2D exchange  $^{13}\text{C}$  NMR spectra of the carboxyl carbon in PEMA.

The coupling of the  $\beta$ -process to the backbone motions was proposed to result from the asymmetric geometry of the ester side group, for which after a simple  $180^\circ$  flip steric problems with adjacent segments arise. With

the plane of the ester side group arranged approximately perpendicular to the local chain axis  $Z$ , this unfavorable interaction can be minimized by a rotation of the backbone around  $Z$ , as sketched schematically in Figure 1a,b, which depict the geometry of the local environment of a PMMA and PEMA segment, respectively. The various isotopically labeled positions used in previous and the current investigations are indicated as well; for the sake of clarity, the methyl group attached directly to the main chain has been drawn on the opposite side of the carboxyl side group. In the current investigation, the unusual mobility of the polymer backbone in the glassy state, which was merely concluded from the NMR spectra of the side group, will be quantified directly by carrying out 2D exchange  $^2\text{H}$  NMR experiments on PMMA and PEMA deuterated at the methyl and methylene moieties of the main chains.

In PEMA, the geometry of motion of the  $\beta$ -relaxation is anisotropic even at elevated temperatures above  $T_g$ , indicating considerable conformational order in the viscoelastic state. Most prominently, this anisotropy leads to a uniaxially averaged one-dimensional (1D)  $^{13}\text{C}$  NMR spectrum of the carboxyl group at 395 K ( $T_g + 55$  K), characterized by a dynamic order parameter of  $S = 0.7$ .<sup>5</sup> Analogously, lower residual ordering was observed in PMMA with  $S = 0.35$  at  $T = T_g + 58$  K, which is comparable to a value recently obtained from residual dipole–dipole couplings in a cross-linked poly(styrene)-*co*-poly(butadiene) (SBR) elastomer.<sup>6</sup> This behavior differs markedly from that of other amorphous polymers, such as atactic polystyrene (PS),<sup>7</sup> where both the backbone and the side group reorient isotropically at similar temperatures above  $T_g$ .

Detailed information about the geometry of the main chain motion in PEMA at a temperature of  $T_g + 20$  K has already been obtained by a difference correlated (DICO) exchange NMR experiment.<sup>8</sup> There, the reorientation dynamics was analyzed quantitatively in terms of a dynamic order parameter  $\langle P_2(t) \rangle = 1/2 \langle 3 \cos^2 \theta(t) - 1 \rangle$ , which is a measure of the loss of orientational

<sup>†</sup> Present address: Department of Chemical Engineering, University of California, Santa Barbara, CA 93106.

<sup>®</sup> Abstract published in *Advance ACS Abstracts*, October 1, 1997.

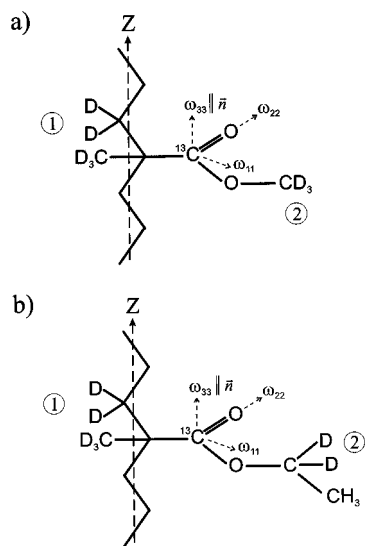


**Figure 1.** (a) Schematic sketch of the geometry of a PMMA segment isotopically labeled at either position: (1) main chain deuterated PMMA- $d_5$  or (2) deuterated at the methoxy side group in PMMA- $d_3$  or  $^{13}\text{C}$  labeled at the carboxyl carbon. In the latter, the orientation of the  $^{13}\text{C}$  chemical shift tensor relative to the local chain axis  $Z$  is indicated, the principal axis  $\omega_{33}$  being approximately parallel to  $Z$  and perpendicular to the plane of the carboxyl group. For clarity, the methyl group attached to the main chain is drawn on the opposite side of the carboxyl side group. (b) As in (a) for a PEMA segment deuterated either at (1) the main chain in PEMA- $d_5$  or (2) PEMA- $d_2$  labeled at the methylene sites of the ethoxy side group.

correlation of a molecular segment at a time  $t$  with respect to its initial orientation at  $t = 0$ . The chain dynamics was found to be bimodal, with pronounced small-angle fluctuations and large-angle reorientations, the latter being associated with conformational transitions. The comparison of the dynamics in PEMA with results obtained for PS<sup>9</sup> revealed that the effective jump angles are smaller in PEMA, inferring higher geometric restrictions in accordance with a higher dynamic anisotropy in PEMA. These results will be discussed in the general context of the dynamics in PEMA as compared to PMMA in the current paper. In particular, the chain motions in PMMA and PEMA will be analyzed directly with respect to the influence of the  $\beta$ -process on the time scale and geometry of the  $\alpha$ -relaxation at and above the glass transition.

For the series of poly(*n*-alkyl methacrylates), a pronounced decrease in the glass transition temperature is observed with increasing length of the alkyl side group.<sup>10,11</sup> This effect, often referred to as internal plasticizing, is attributed to an increase in distance between adjacent polymer chains, which results in a higher mobility of the backbone itself. Differently, the correlation times of the  $\beta$ -process, despite the increasing size of the side group, are roughly similar in dielectric measurements with their activation energies increasing slightly<sup>10</sup> with alkyl side chain length or found to be nearly identical in dynamic mechanic measurements.<sup>12</sup> Therefore, the investigation of higher methacrylate polymers, such as PEMA, provides insight into the effect of the dynamics of the larger and therefore even more asymmetric ester side groups on the characteristics of the  $\alpha$ -relaxation.

## II. Solid-State NMR Spectroscopy

In solids, the couplings of nuclear spins with their local surroundings are anisotropic, leading to inhomogeneous

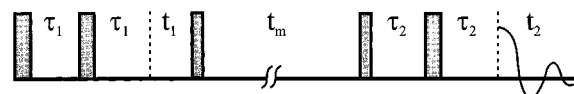


**Figure 2.** Pulses and time periods for the five-pulse sequence of the 2D exchange  $^2\text{H}$  NMR experiment. The angular dependent NMR frequency is encoded during the evolution time  $t_1$ , and the information about molecular orientation is preserved as longitudinal magnetization in the following mixing time  $t_m$ . The frequencies after  $t_m$ , which generally differ from those during  $t_1$  when molecular reorientations in  $t_m$  take place, are read out in the detection time  $t_2$ . In both evolution and detection periods a refocusing pulse is inserted, analogous to the one-dimensional solid-echo pulse sequence, with time delays  $\tau_1$  and  $\tau_2$ , respectively. By incrementing  $t_1$ , a two-dimensional time domain data set is obtained, which after a double Fourier transform yields the 2D exchange spectrum.

geneously broadened NMR spectra.<sup>4</sup> In particular, solid-state  $^2\text{H}$  NMR exploits the anisotropic coupling of the quadrupole moment of the  $^2\text{H}$  nucleus with an electric field gradient (EFG) tensor at the nuclear site. For aliphatic moieties, the EFG tensor is approximated to be axially symmetric with the unique axis along the  $\text{C}-^2\text{H}$  bond; in this case, the angular dependence of the NMR frequency  $\omega_{\pm}(\vartheta)$  of a molecular site is given by<sup>4</sup>

$$\omega_{\pm}(\vartheta) = \omega_0 \pm \frac{1}{2}\delta(3 \cos^2 \vartheta - 1) \quad (1)$$

where the polar angle  $\vartheta$  describes the orientation of the  $\text{C}-^2\text{H}$  bond with respect to the external magnetic field  $\mathbf{B}_0$ . Here,  $\omega_0$  denotes the Larmor frequency, and the anisotropy parameter  $\delta$  specifies the strength of the quadrupolar interaction. Thus, the orientation of a molecular segment is directly related to the position of a line in the resulting one-dimensional spectrum; and, for an isotropic distribution of sites, a powder pattern (Pake spectrum) is observed.

Reorientations render  $\vartheta$  and thus  $\omega(\vartheta)$  time dependent, with motions on a time scale of microseconds or faster resulting in characteristic changes of the one-dimensional  $^2\text{H}$  NMR line shape. For example, the fast rotation of a methyl group about its  $C_3$  symmetry axis gives rise to a motionally averaged Pake spectrum, scaled by an averaged anisotropy parameter  $\bar{\delta} = -1/3\delta$ , with the unique axis of the EFG tensor pointing along the  $C_3$  axis.

Unique geometric information about microscopic molecular motions on a time scale of milliseconds to seconds is accessible by 2D exchange solid-state NMR spectroscopy, which probes the orientation of a particular site at two subsequent times. The relevant pulses and time periods of the 2D exchange  $^2\text{H}$  NMR experiment are shown in Figure 2. Transverse magnetization is created during the evolution time  $t_1$ , which encodes the angular dependent frequency of a particular site, i.e., a  $\text{C}-^2\text{H}$  bond orientation. While this information is retained as longitudinal magnetization in the following mixing time  $t_m$ , molecular reorientations in  $t_m$  may lead to a change of frequencies, and the new frequencies are read out in the subsequent detection period  $t_2$ . Analogous to the solid-echo pulse sequence in one-dimensional  $^2\text{H}$  NMR, a refocusing  $\pi/2$  pulse is applied, preceding both the evolution and detection periods to overcome experimental difficulties due to receiver dead time and finite pulse lengths.<sup>13,14</sup> Incrementing the evolution time  $t_1$  leads to a 2D time domain data set, from which the 2D spectrum is obtained by a double Fourier transform. With  $t_1, t_2 \ll t_m$  and correlation times  $\tau_c$  of the dynamic process on the order of the

mixing time, no frequency changes during the evolution and detection periods are present (slow motion limit). Then the 2D spectrum represents the conditional probability of finding a molecular segment at a particular frequency  $\omega_2$  in the detection period  $t_2$ , given it had the frequency  $\omega_1$  in the evolution period  $t_1$ ; and, by parametrically varying  $t_m$ , the dynamic process can be followed in real time.

For discrete jump motions during the mixing time, the 2D spectrum exhibits characteristic elliptical exchange ridges and allows a direct and model-free extraction of the reorientation angle  $\beta$ , that is, the relative angle of a given C—H bond before and after the jump. For a broad distribution of reorientation angles, often encountered in conjunction with a distribution of correlation times for the dynamics in amorphous polymers, the exchange intensity can be visualized as being composed of a superposition of the ellipses for the various reorientation angles, which smears out the distinctive features of the exchange spectra, giving them overall the appearance of a diffusive type of motion. While small-angle fluctuations essentially cause a broadening of the diagonal spectrum, which by itself indicates that no reorientation has occurred during the mixing time (and hence  $\omega_1 = \omega_2$ ), diffusive-type large-angle motions lead to exchange intensity spread out over the entire spectral 2D plane. In this case, the analysis of the 2D spectra to extract the geometry and correlation time of motion often relies on the comparison of the experimental spectra with those simulated for various motional models. In the past, isotropic rotational diffusion,<sup>15</sup> i.e., small-step diffusion on a sphere, together with a distribution of correlation times has been successfully applied to quantify the reorientation dynamics of amorphous polymers near the glass transition, such as, for example, polystyrene<sup>7</sup> (PS), atactic polypropylene<sup>16</sup> (aPP), and polyisoprene<sup>17</sup> (PI). However, at higher temperatures above  $T_g$ , a model of isotropic random jumps has led to a better agreement with experimental spectra of PI than did isotropic rotational diffusion.

In the analysis of 2D exchange NMR spectra, a series of mixing time dependent spectra must be compared with the corresponding simulations for different motional models, since a single 2D spectrum does not yield unique parameters to characterize the molecular motions. Alternatively in amorphous polymers, a model-free approach in terms of dynamic order parameters, focusing on the detailed geometry of motion and the separation of small-angle and large-angle motions, has been successfully applied to PEMA<sup>8</sup> and PS.<sup>9</sup> However, to elucidate the general features of the spectra in terms of the geometry of motion, as well as of the correlation times and distribution width, it is advantageous to record 2D exchange spectra.

Furthermore, not only the broad distribution of reorientation angles but also the large width of the distribution of correlation times has to be taken into account when analyzing polymer dynamics. For average correlation times of a few milliseconds having a distribution several decades wide, the assumption of the slow motion limit in the simulations of the exchange NMR spectra is no longer justified, and frequency changes during all time intervals of the 2D experiment must be considered. With correlation times being in the intermediate dynamic regime, the 2D spectrum can no longer be identified with a two-time distribution function, because it now depends on the reorientation path

of the molecules in the evolution and detection periods as well. Since the time domain 2D signals for the three- and four-pulse sequence in the intermediate motional regime have already been derived,<sup>18</sup> only a brief discussion with respect to the application to the five-pulse sequence, shown in Figure 2, will be presented here.

In the slow motion limit (sml), the complex 2D time domain signal, which depends on the variables  $t_1$ ,  $t_2$ , and, for a given 2D exchange experiment parametrically on  $t_m$ , is given by the expression

$$G_{\pm}^{\text{sml}}(t_1, t_2; t_m) = \langle 1 | \exp(\pm i\omega_2 t_2) \exp(\mathbf{\Pi} t_m) \exp(i\tilde{\omega}_1 t_1) \mathbf{W} | 1 \rangle \quad (2)$$

Here,  $\langle 1 |$  is a unit row vector,  $|1\rangle$  its transposed column vector, and  $\tilde{\omega}_1$  and  $\tilde{\omega}_2$  are diagonal matrices with elements that denote the NMR frequencies during the evolution time and detection time, respectively.  $\mathbf{\Pi}$  is the exchange matrix with elements  $\Pi_{jk}$  associated with orientation changes from a state  $k$  to a state  $j$  (e.g., a tridiagonal matrix for rotational diffusion), and  $\mathbf{W}$  is a diagonal matrix with elements  $W_{kk}$  describing the *a priori* probabilities of finding the system in a particular orientational state  $k$ . In 2D <sup>2</sup>H NMR, the experimentally measured cosine and sine modulated data sets  $F_{\text{cos,cos}}$  and  $F_{\text{sin,sin}}$ , from which the purely absorptive 2D exchange NMR spectrum is obtained by a 2D Fourier transformation and appropriate combination of the two resulting spectra, are related to the complex 2D time domain signal  $G_{\pm}$  by

$$F_{\text{cos,cos}} = \frac{1}{2} \text{Re}(G_- + G_+) \quad (3)$$

$$F_{\text{sin,sin}} = \frac{1}{2} \text{Re}(G_- - G_+) \quad (4)$$

The 2D signal for the five-pulse sequence for the general case<sup>18</sup> (gen) is obtained by taking into account the effects of frequency changes during all periods of the experiment, i.e., the mixing time  $t_m$ , evolution and detection times  $t_1$  and  $t_2$ , respectively, and the refocusing times  $\tau_1$  and  $\tau_2$ , as indicated in Figure 2. The effect of the refocusing times can be treated in an analogous manner to the calculation of the 1D time domain signal for the solid-echo (SE) pulse sequence. With  $\tau$  being the time interval between the two pulses and the refocusing time after the second pulse, and  $t_2$  starting from the echo maximum, the 1D signal  $G_{\text{SE}}(t_2; \tau)$  in the intermediate dynamic regime is calculated as<sup>19</sup>

$$G_{\text{SE}}(t_2; \tau) = \langle 1 | \exp((\mathbf{\Pi} - i\omega) t_2) \exp((\mathbf{\Pi} - i\omega) \tau) \times \exp((\mathbf{\Pi} + i\omega) \tau) \mathbf{W} | 1 \rangle \quad (5)$$

Thus, combining eqs 2 and 5 to account for the dynamics also during the evolution and detection periods, one arrives at the expression for the five-pulse sequence  $G_{\pm}^{\text{gen}}(t_1, t_2; \tau_1, \tau_2, t_m)$  for the general case

$$G_{\pm}^{\text{gen}}(t_1, t_2; \tau_1, \tau_2, t_m) = \langle 1 | \exp((\mathbf{\Pi} \pm i\omega) t_2) \times \exp((\mathbf{\Pi} \pm i\omega) \tau_2) \exp((\mathbf{\Pi} \mp i\omega) \tau_2) \exp(\mathbf{\Pi} t_m) \times \exp((\mathbf{\Pi} - i\omega) t_1) \exp((\mathbf{\Pi} - i\omega) \tau_1) \exp((\mathbf{\Pi} + i\omega) \tau_1) \mathbf{W} | 1 \rangle \quad (6)$$

By setting  $\tau_1 = \tau_2$ , symmetric spectra with respect to the main diagonal ( $\omega_1 = \omega_2$ ) and subdiagonal ( $\omega_1 = -\omega_2$ ) are obtained, in contrast to 2D spectra acquired with the four-pulse sequence, where the only refocusing pulse

**Table 1. Number-Averaged and Weight-Averaged Molecular Weights  $M_n$  and  $M_w$ , Respectively, Polydispersities  $M_w/M_n$ , and Glass Transition Temperatures  $T_g$  of the Investigated PMMA and PEMA Samples Obtained by GPC and DSC, Respectively<sup>a</sup>**

sample	$M_n$ (g/mol)	$M_w$ (g/mol)	$M_w/M_n$	$T_g$ (K)	
PMMA- $d_5$	$[-CD_2C(CD_3)(COOCH_3)]_n$	68 300	124 500	1.83	398
PMMA- $d_3$	$[-CH_2C(CH_3)(COOCD_3)]_n$	48 800	94 500	1.94	395
PMMA- $^{13}COOR$	$[-CH_2C(CH_3)(^{13}COOCH_3)]_n$	55 500	112 000	2.02	401
PEMA- $d_5$	$[-CD_2C(CD_3)(COOCH_2CH_3)]_n$	76 400	105 700	1.38	345
PEMA- $d_2$	$[-CH_2C(CH_3)(COOCD_2CH_3)]_n$	68 900	117 500	1.71	349
PEMA- $^{13}COOR$	$[-CH_2C(CH_3)(^{13}COOCH_2CH_3)]_n$	54 500	120 000	2.2	340

<sup>a</sup> For comparison, the data of the samples investigated previously are also included.

**Table 2. Stereoregularity of the Various Polymers As Obtained by High-Resolution  $^1H$  and  $^{13}C$  NMR**

sample		triads		
		<i>mm</i>	<i>mr</i>	<i>rr</i>
PMMA- $d_5$	$[-CD_2C(CD_3)(COOCH_3)]_n$	0.04	0.32	0.64
PMMA- $d_3$	$[-CH_2C(CH_3)(COOCD_3)]_n$	0.03	0.35	0.62
PMMA- $^{13}COOR$	$[-CH_2C(CH_3)(^{13}COOCH_3)]_n$	0.06	0.32	0.62
PEMA- $d_5$	$[-CD_2C(CD_3)(COOCH_2CH_3)]_n$	0.11	0.31	0.58
PEMA- $d_2$	$[-CH_2C(CH_3)(COOCD_2CH_3)]_n$	0.04	0.43	0.53
PEMA- $^{13}COOR$	$[-CH_2C(CH_3)(^{13}COOCH_2CH_3)]_n$	0.03 (0.02) <sup>a</sup>	0.35	0.62

sample		pentads				
		<i>mrrm</i>	<i>mrrr</i>	<i>rrrr</i>	<i>mrrm + mrrr</i>	<i>mrrr + rrrr</i>
PEMA- $d_5$	$[-CD_2C(CD_3)(COOCH_2CH_3)]_n$	0.04	0.21	0.39	0.07	0.27

<sup>a</sup> Determined from the carboxyl carbon  $^{13}C$  NMR resonance.

before the detection period may break the  $C_{2v}$  symmetry of the 2D  $^2H$  NMR spectrum. Details of the simulations and numerical aspects thereof can be found in ref 18.

### III. Experimental Section

**NMR.**  $^2H$  NMR spectra were recorded on Bruker CXP 300 and ASX 500 spectrometers, operating at resonance frequencies of 45 MHz and of 76.8 MHz, respectively. For the 1D spectra, the solid-echo pulse sequence was used with 90° pulse lengths ranging between 2.5 and 3.0  $\mu s$ , a delay time of 20  $\mu s$  between the pulses, and the total spectral width set to 1 MHz. For the 2D exchange spectra, the five-pulse sequence shown in Figure 2 was employed to record the cosine and sine modulated data sets, with delay times of 20  $\mu s$  for the echo sequences preceding the evolution and detection times. The dwell time in both dimensions was set to 3.2  $\mu s$ , corresponding to a total spectral width of 312 kHz. Generally, 256 complex data points were acquired in the detection times. In the indirect dimension, between 35 and 60 increments were taken and zero-filled to yield a symmetric data matrix prior to Fourier transforms. Data processing of the cosine and sine data set to obtain purely absorptive spectra was accomplished as described in the literature.<sup>13,14</sup> The recycle delay was set to at least 2.5 times the longest spin–lattice relaxation time observed; resulting in measuring times for a 2D exchange spectrum typically between 12 and 24 h.

**Synthesis and Polymerization of the Deuterated PMMA and PEMA Samples.** Main chain deuterated PMMA- $d_5$  was obtained following the procedure described earlier.<sup>2</sup> Starting from acetone- $d_6$  and NaCN, acetone cyanhydrin was formed in the presence of  $D_2SO_4$ , and, by elimination of water, acetonitrile- $d_5$  was obtained (yield ~ 80%). Saponification of the nitrile and esterification with methanol gave methyl methacrylate- $d_5$  in a yield of about 60%. PEMA- $d_5$  was obtained analogously by reacting ethanol in the esterification step, while for the synthesis of the side chain labeled PEMA- $d_2$  starting from acetone, ethanol- $d_2$  was used in the esterification step. The monomers were polymerized with 0.5 mol % azobis(isobutyronitrile) as initiator in toluene at 60 °C, and resulting polymers were precipitated from methanol for purification with a yield of about 70%.

**Characterization.** The number-averaged and weight-averaged molecular weights  $M_n$  and  $M_w$ , respectively, of the PMMA and PEMA samples were obtained by GPC using PMMA as a standard, and are summarized in Table 1, together with the polydispersities ( $M_w/M_n$ ) and glass transition tem-

peratures as measured by DSC at a heating rate of 10 K/min. The tacticities were obtained by high-resolution  $^1H$  and  $^{13}C$  NMR at 500.13 and 125.76 MHz, respectively, and are presented in Table 2. In PMMA- $d_5$ , the  $^1H$  NMR methoxy resonances in chlorobenzene- $d_5$  at 373 K were used for the triad analysis.<sup>20</sup> For the PEMA samples, nitrobenzene- $d_5$  was used as a solvent at a temperature of 353 K. While in PEMA- $d_5$ , the triads and pentads were obtained from  $^{13}C$  NMR of the quaternary carbon at the backbone and the carboxyl carbon,<sup>21</sup> the  $^1H$  NMR main chain methyl resonances were analyzed in PEMA- $d_2$ .<sup>20</sup> For comparison, the data of the  $^{13}C$ -labeled samples and PMMA- $d_3$  investigated previously<sup>2,3</sup> are included in the tables as well.

### IV. Results and Discussion

**A. Dynamics in the Glassy State.** To probe directly the restricted backbone motion, which was proposed from  $^{13}C$  NMR spectra of the side group,<sup>2,3</sup> 2D exchange  $^2H$  NMR spectra of PEMA- $d_5$  (see Figure 1b) were recorded at a temperature of 335 K ( $T_g - 10$  K), where the correlation time of the  $\beta$ -relaxation is approximately 10 ms.<sup>3</sup> Spectra for mixing times of 50 and 500 ms are shown in Figure 3a (left column). Along the diagonal, which represents segments that did not change their orientation during the mixing time  $t_m$ , a superposition of the motionally averaged and partially relaxed methyl spectrum and the full-width methylene spectrum appears. The diagonal components in the spectra acquired for the two different mixing times exhibit considerable broadening, which extends into the 2D plane and can be best seen along the “90° ridge” of the outer singularities corresponding to the methylene spectrum. The extent by which the ridges reach out into the 2D plane indicates that reorientation by as much as 50° has taken place in the course of both mixing times. Yet, it is apparent that the exchange intensity does not increase in extent or amount with mixing time, demonstrating directly that the molecular potential remains unchanged on a time scale which by far exceeds the correlation time of the  $\beta$ -process.

In the spectrum with  $t_m = 50$  ms, the methyl group spectrum already has less intensity than expected from the integral ratio of 3:2 for the methyl versus the

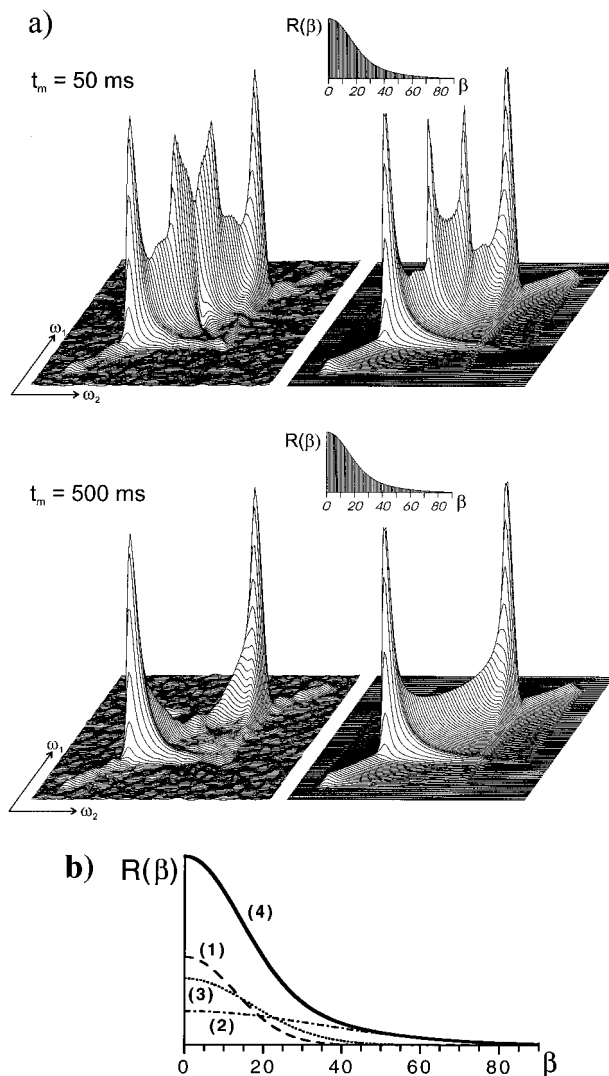


**Figure 3.** (a) 2D exchange  $^2\text{H}$  NMR spectra (left) of PEMA- $d_5$  at  $T = 335\text{ K}$  ( $T_g - 10\text{ K}$ ) at the indicated mixing times ( $t_m$ ). The spectra exhibit considerable spectral intensity away from the diagonal even below  $T_g$ , caused by a restricted rotation of main chain segments coupled to a  $180^\circ$  flip of the carboxyl side group ( $\beta$ -relaxation) in a constant molecular potential. The corresponding simulations (right column) and reorientation angle distributions  $R(\beta)$ , shown as insets, are based on a superposition of Gaussian distributions shown in Figure 3b, which were proposed from the mechanism of the  $\beta$ -relaxation. (b) Construction of the jump angle distributions  $R(\beta)$  of Figure 3a from three Gaussian distributions around the equilibrium position of  $\beta = 0$ , according to the three underlying motional processes. Component 1 corresponds to main chain segments that undergo merely a rocking motion of  $30^\circ$  fwhm, while component 2 with  $80^\circ$  fwhm and component 3 with  $40^\circ$  fwhm result from segments performing an odd number of carboxyl side group flips or have nearly returned to their initial position after an even number of flips, respectively. Component 4 shows the resulting shape of  $R(\beta)$  used for the simulations in Figure 3a.

methylene spectrum. This is due to longitudinal relaxation during the mixing time being much faster for the methyl deuterons than for the methylene deuterons; and the relaxing portion is removed from the spectrum by proper phase cycling of the pulses in the five-pulse sequence.<sup>4,14</sup> In addition, the anisotropies of  $T_1$  and  $T_{1Q}$ , corresponding to the longitudinal relaxation times of the cosine and sine modulated 2D data sets, respectively, cause distortions in the line shape and also a relaxation ridge along the subdiagonal. After 500 ms, only the methylene spectrum remains, while the methyl group

spectrum is completely relaxed with its intensity phase-cycled away, leaving an apparent negative intensity, as visible in the center of the methylene spectrum on the diagonal. This effect is most likely due to the onset of spin diffusion<sup>4</sup> from the methylene deuterons to the methyl deuterons. Spin diffusion is most efficient when the overlap of the resonance lines is maximized; in this case the magnetization is transported from the methylene deuterons to the methyl deuterons, where it relaxes during the mixing time and its contribution is subsequently removed by the phase cycling.

The simulations of the 2D spectra in Figure 3a (right column) and the corresponding reorientation angle distribution  $R(\beta)$ , shown as insets, were calculated by considering the polymer microstructure as investigated by wide-angle X-ray scattering (WAXS),<sup>22</sup> which was used to probe the local conformation of atactic PMMA. From the comparison of experimental and calculated X-ray diffraction patterns, a preference for the all-trans conformation with an average length of 16–20 backbone bonds was concluded. In accordance with rotational isomeric state (RIS) models of syndiotactic PMMA,<sup>23</sup> the plane of the carboxyl side group is essentially perpendicular to the backbone axis  $Z$ , and the  $\text{C}-\text{OCH}_3$  bond is in the trans conformation with respect to the  $\text{C}-\text{C}$  bond connecting the backbone and the ester side group. For a gauche conformation, the angle of the carboxyl plane with the local chain axis  $Z$  deviates by  $30\text{--}40^\circ$  from that of the trans conformation, but the normal vector  $\vec{n}$  of the carboxyl plane remains still approximately parallel to the particular gauche backbone bond. Therefore, to a good approximation, the  $\text{C}-^2\text{H}$  bonds of the methylene groups and the  $\text{C}_3$  symmetry axes of the main chain methyl groups are perpendicular to the local chain axes, as is the case for the planes of the carboxyl side groups; see Figure 1a,b.

The reorientation angle distribution  $R(\beta)$  (Figure 3a, insets, and Figure 3b) was calculated as proposed from the different geometries of motion determined from the carboxyl side group  $^{13}\text{C}$  NMR spectra.<sup>2,3</sup> The composition of the shape of  $R(\beta)$  as a superposition of three Gaussian distributions around the equilibrium position of  $\beta = 0$  is demonstrated in Figure 3b, with the characteristics of the different components as follows: 20% of the backbone segments (component 1) do not participate in the ester side group flip and only undergo rocking motions of  $30^\circ$  (full width at half-maximum, fwhm). Further, 40% of the main chain segments respond to a  $180^\circ$  flip process (or any other odd number of flips) of the ester side group and make up component 2, rocking with a distribution of  $80^\circ$  fwhm, which corresponds to the "tail" toward large  $\beta$  in the reorientation angle distribution in Figure 3a. The remaining 40% are found in their original position (component 3) with an imprecision of  $40^\circ$  fwhm after an even number of jumps, this distribution being caused by the asymmetry of the carboxyl side group. In summary, the shape of  $R(\beta)$ , marked as component 4 and shown as insets in Figure 3a, results.

The distribution width is found to be slightly larger than observed for the main chain reorientation of PMMA- $d_5$  below the glass transition temperature,<sup>24</sup> and about  $20\text{--}30^\circ$  larger as proposed from the 2D exchange  $^{13}\text{C}$  NMR spectra of PEMA at room temperature<sup>3</sup> (note that in ref 3, the rocking motion was given as  $\pm 20^\circ$  rms amplitude, which is equal to a distribution width of  $47^\circ$  fwhm). Furthermore, the 2D exchange  $^{13}\text{C}$  NMR spectra of PEMA at room temperature indicated a smaller

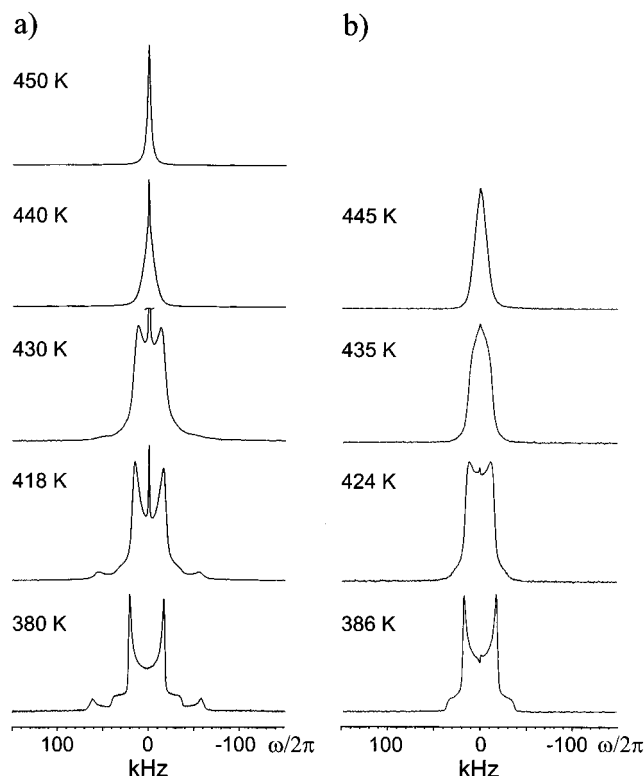


**Figure 4.** (a) 1D solid-echo NMR spectra of main chain deuterated PMMA- $d_5$ , consisting of a superposition of the inner methyl and outer methylene spectra, as a function of temperature below and above the glass transition temperature ( $T_g = 398$  K). Above  $T_g$ , the line shapes are characteristic of a broad distribution of reorientation angles and correlation times, and the spectrum is narrowed to a broadened isotropic line at 450 K. (b) 1D solid-echo NMR spectra of the motionally narrowed methoxy deuterated PMMA- $d_3$  ( $T_g = 395$  K). The spectra are similar to those of PMMA- $d_5$ , because the orientation of the tensor axis of the methoxy group is parallel to the flip axis of the carboxyl group, and is thereby invariant under the  $\beta$ -process; and consequently, PMMA- $d_3$  may be used as a probe for main chain reorientations.

total fraction of about 40% of carboxyl side groups participating in the  $180^\circ$  flip motions.

The increased bulkiness of the side group alkyl chain in PEMA does not seem to be the primary cause for the increased amount of exchange intensity and larger distribution width observed in the  $^2\text{H}$  NMR spectra, since both the 2D exchange  $^{13}\text{C}$  NMR spectra of PMMA and PEMA exhibit the same distribution of reorientation angles at about 40 K below their respective glass transitions. Instead, the PEMA spectra are indicative of an additional higher mobility, present already below  $T_g$ , of the main chain than in PMMA, for which the reorientation angle distribution remains constant in the glassy state.<sup>24</sup> In the higher homologue poly(*n*-butyl methacrylate) (PnBMA), this effect is even more pronounced and manifests itself in a very slow main chain motion just below  $T_g$ , as observed by high-resolution 2D exchange  $^{13}\text{C}$  NMR spectra of the carboxyl group.<sup>25</sup>

**B. Dynamics at the Glass Transition. One-Dimensional Spectra of PMMA and PEMA.** To probe the general dynamic behavior in PMMA and PEMA, one-dimensional  $^2\text{H}$  NMR spectra were recorded as a function of temperature. Figure 4a shows the 1D solid echo spectra of PMMA- $d_5$  between 380 and 450 K. The spectrum at 380 K, 18 K below the glass transition temperature, consists of the superposition of the inner methyl and outer methylene subspectra with an integral intensity ratio of 3:2 and quadrupole splittings of  $\delta =$

$2\pi \times 38$  kHz and  $\delta = 2\pi \times 120$  kHz, characteristic of fast rotating methyl groups and rigid aliphatic species, respectively. Above  $T_g$ , at a temperature of 418 K, a slight decrease in the values of  $\delta$  to approximately  $2\pi \times 32$  kHz and  $2\pi \times 112$  kHz is observed, as well as deviations from the static powder line shapes, in conjunction with a reduction of the methylene signal intensity, indicating motional correlation times in the intermediate motional regime.<sup>19</sup> At even higher temperatures, a broadened signal of only the methyl group is visible, since due to its larger anisotropy parameter, the methylene signal intensity is affected more strongly by the dynamics. The line shape of the methyl group in this temperature range is characteristic of a motion with a broad distribution of reorientation angles and correlation times, as observed previously in other amorphous polymers.<sup>7</sup> At 450 K, the signal consists of a slightly broadened isotropic line, the correlation times now being almost in the fast motion limit ( $\tau_c \leq 1$   $\mu\text{s}$ ). Similar spectra of fully deuterated and main chain deuterated PMMA have been reported previously.<sup>26</sup>

For comparison, in Figure 4b the 1D spectra of PMMA- $d_3$  ( $T_g = 395$  K) are shown, which display the same temperature dependence of their line shapes as PMMA- $d_5$  and a similar reduction of the quadrupole splitting of the methyl group from  $2\pi \times 35$  kHz at 386 K to  $2\pi \times 32$  kHz at 424 K. The  $C_3$  symmetry axis of the methoxy group is parallel to the flip axis of the side group, as demonstrated by static 2D exchange  $^{13}\text{C}$  NMR experiments involving spin diffusion<sup>27</sup> between the doubly  $^{13}\text{C}$  labeled carboxyl and methoxy carbon, and 2D exchange  $^2\text{H}$  NMR spectra of the methoxy group below  $T_g$ .<sup>2</sup> Thus, with the orientation of the methoxy group being invariant under the  $\pi$ -flip motion of the  $\beta$ -relaxation itself, the deuterated methoxy moiety sensors the main chain dynamics below and above  $T_g$ .

The overall line shapes of the 1D spectra of main chain deuterated PEMA- $d_5$  in Figure 5a, acquired at different temperatures above the glass transition, are similar to those in PMMA, yet with a weaker temperature dependence for PEMA. At 365 K ( $T_g + 20$  K), the static quadrupole splittings of  $2\pi \times 119$  kHz and  $2\pi \times 37$  kHz are observed for the methylene and methyl subspectra, respectively, and changes in the 1D line shapes become prominent around 402 K, leading to a smaller quadrupole splitting and reduced intensity of the spectrum. At about the same temperature (395 K =  $T_g + 55$  K), a uniaxially averaged one-dimensional  $^{13}\text{C}$  NMR spectrum of the carboxyl group is observed,<sup>5</sup> caused by a rapid averaging of the chemical shift tensor components perpendicular to the local chain axis due to the  $\beta$ -process and rotation around Z, while the parallel tensor component remains nearly invariant on a fast time scale. In the  $^2\text{H}$  NMR spectra of PEMA- $d_5$ , the motions parallel and perpendicular to the local chain axis are not by themselves discernible due to the uniaxiality of the EFG tensor of the C- $^2\text{H}$  bond. The one-dimensional  $^2\text{H}$  NMR line shapes, however, indicate slower reorientations of the polymer backbone with a distribution of correlation times on the intermediate (microsecond) and slow (millisecond) time scale, which in conjunction with the one-dimensional  $^{13}\text{C}$  and  $^2\text{H}$  line shapes demonstrates that the mobility perpendicular to the backbone is much faster than the reorientation of the chain axis itself. At higher temperatures, further narrowing is observed in the 1D  $^2\text{H}$  NMR spectra, resulting in an isotropic line at 435 K, which corresponds to a reduced temperature  $T^* = T/T_g = 1.26$ , as

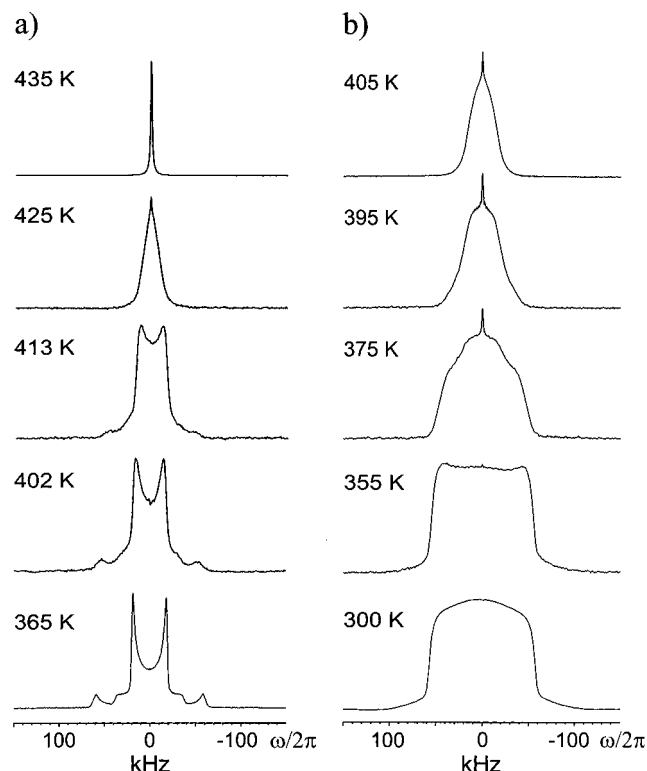


**Figure 5.** (a) Temperature dependent 1D solid-echo NMR spectra of main chain deuterated PEMA- $d_5$  ( $T_g = 345$  K), consisting of a superposition of the inner methyl and outer methylene spectra, which although similar to the spectra of PMMA- $d_5$  shown in Figure 4a, demonstrate a weaker temperature dependence of backbone motions above the glass transition. (b) 1D solid-echo NMR spectra of PEMA- $d_2$ , labeled at the methylene site of the ethoxy side group, which shows a high mobility already below  $T_g$ , caused by the  $\gamma$ -relaxation, while above  $T_g$  the line shapes are influenced by both the  $\beta$ - and  $\gamma$ -processes.

compared to PMMA, where a single line is observed around  $T^* = 1.13$ . In summary, the chain motion in PEMA is markedly slower than in PMMA.

At room temperature, the ethyl side group is already highly mobile, with the broad square-shape spectrum of PEMA- $d_2$  of fwhm  $2\pi \times 110$  kHz, suggesting a hindered rotation around the C- $CD_2(CH_3)$  bond on a microsecond time scale; see Figure 5b. The correlation time of the  $\beta$ -process is approximately 200 ms at this temperature, and hence, this process cannot account for the observed 1D line shapes. These result from the  $\gamma$ -relaxation, a local segmental motion of the alkyl side group.<sup>11</sup> Above  $T_g$ , the 1D line shapes are mainly influenced by both the  $\gamma$ - and  $\beta$ -processes, which approach the fast motion limit at a temperature of about 400 K. The line shape observed at  $T = 405$  K again indicates that apart from the dynamics induced by the  $\beta$ -process, together with the rocking motion around the main chain axis, an additional rotation around the C- $CD_2(CH_3)$  bond takes place. The half-width of about  $2\pi \times 30$  kHz is not in accord with a mere  $180^\circ$  jump motion of the carboxyl group ( $\beta$ -process), which would lead to an averaged asymmetry parameter of  $\bar{\eta} = 1$  and an averaged anisotropy parameter of  $\bar{\delta} = 1/2\delta_{\text{methylene}}$  (kink spectrum).

Similarly, line shape distortions in a dipolar powder pattern of the ethoxy group,  $^{13}C$ -labeled at both carbons, were ascribed to a significant mobility of the ethyl side group at room temperature and could be only frozen out at 170 K.<sup>27</sup> At this temperature, the most likely side

chain conformation, found by correlating the dipole-dipole interaction with the  $^{13}C$  chemical shift anisotropy, was found to be planar all-trans.

**2D Exchange Spectra of PEMA.** As estimated from the one-dimensional spectra of PEMA, the temperature range where two-dimensional NMR methods are applicable extends approximately to  $T_g + 50$  K. To monitor the onset of the  $\alpha$ -relaxation, a series of 2D exchange  $^2H$  NMR spectra of PEMA- $d_5$  was recorded as a function of mixing time at 355 K, 10 K above the glass transition temperature. In the spectra shown in Figure 6 (left columns, respectively), it is immediately visible that the exchange intensity is confined to the vicinity of the diagonal at a relatively short mixing time of 20 ms, while with longer mixing times  $t_m$  increase in intensity and slowly spread out into the entire 2D plane until the diagonal intensity has completely vanished at  $t_m = 500$  ms. As was already the case in the glassy state, the fast and anisotropic  $T_1$  and  $T_{1Q}$  relaxations of the methyl groups cause a relative decrease of the intensity of the corresponding line shape as well as line shape distortions of the inner part of the spectrum.

Clearly, contrary to the observations in the glassy state, above  $T_g$  the molecular potentials are changing with time, caused by main chain reorientations not primarily associated with the  $180^\circ$  flip of the carboxyl group, since for the flip motion the correlation times are less than 1 ms at the respective temperatures. Assuming a predominantly trans conformation for the mainly syndiotactic sequences of the polymer backbone as discussed above, the absence of any characteristic exchange ridge and the diffusive appearance of the 2D  $^2H$  NMR spectra, together with the anisotropic character of the  $\beta$ -process above the glass transition, suggest a planar rotational diffusion of main chain segments around the local chain axis  $Z$  (i.e., a diffusion on a cone with the central axis along  $Z$  and a semiangle of  $90^\circ$ ), eventuating in a uniform distribution of segments in a plane. Stated differently, caused by the onset of the  $\alpha$ -relaxation, the equilibrium positions of the backbone rocking motions of the  $\beta$ -process become increasingly imprecise after a large number of side group flips, overall resulting in a slow rotation of the main chain itself. The corresponding reorientation angle distribution  $R(\beta)$  is a one-dimensional Gaussian distribution with a variable width defined in the angular range of  $0^\circ \leq \vartheta \leq 180^\circ$ . Since from the angular dependence of the NMR frequency in eq 1, angles of  $\vartheta$  and  $180^\circ - \vartheta$  cannot be distinguished, only the even parts of  $R(\beta)$  in the interval  $0^\circ \leq \vartheta \leq 90^\circ$  are shown as insets in Figure 6.

The simulations for a planar rotational diffusion, shown in Figure 6 (right column), agree well with the experimental spectra for the corresponding mixing times if the correlation time for planar diffusion is chosen to be  $\tau_c = 600 \pm 200$  ms. However, the diagonal intensity in the experiment for the longest mixing time of 500 ms is less than in the corresponding simulation, which can be explained either by the  $\beta$ -process being in the intermediate motional regime, thus causing an additional loss of diagonal intensity due to the concomitant main chain rocking motion or by deviations from the ideal planar rotation with time, originating from, for example, conformational transitions. Furthermore, as explained earlier, the magnetization transfer to the fully relaxed methyl group may lead to an additional reduction of diagonal intensity.



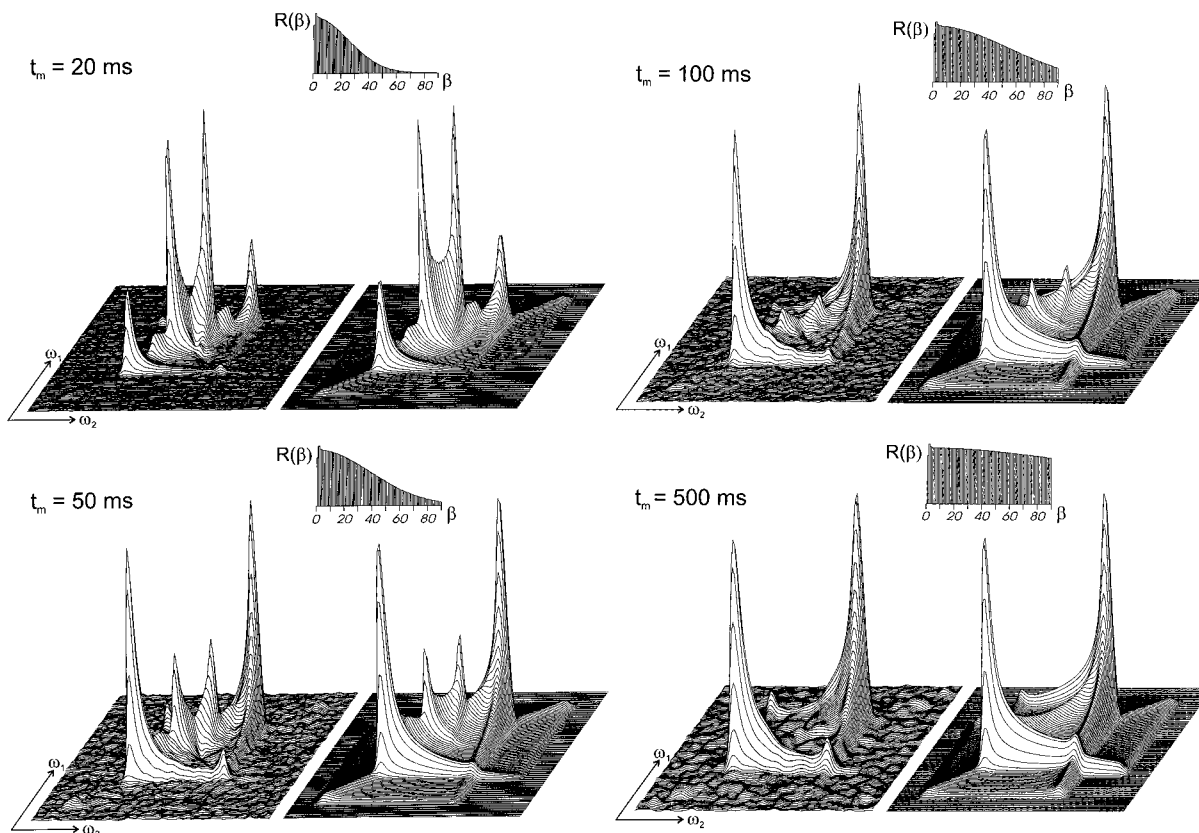


**Figure 6.** 2D exchange  $^2\text{H}$  NMR spectra (left columns, respectively) of PEMA- $d_5$  at 355 K ( $T_g + 10$  K) and the indicated mixing times. The spreading of the featureless exchange intensity with mixing time, equivalent to increased reorientation angles, demonstrates a changing dynamic molecular potential for each C- $^2\text{H}$  bond. The anisotropic character of the  $\beta$ -relaxation above  $T_g$  influences the motional geometry of the  $\alpha$ -relaxation, leading to a rotation of main chain segments around the local chain axis  $Z$ ; see Figure 1b. The simulations (right columns, respectively) and Gaussian reorientation angle distributions  $R(\beta)$  (insets) are based on the model of planar diffusion about  $Z$  with a correlation time  $\tau_c = 600$  ms.

Neither incorporating a distribution of correlation times for planar diffusion nor the change to the motional model of an isotropic rotational diffusion improves the fits: Choosing a small distribution width of correlation times for isotropic rotational diffusion, too much exchange intensity is observed in the experimental spectra for intermediate and longer mixing times, whereas for a broad distribution of correlation times the diagonal intensity in the simulation remains too high, also in disagreement with the experimental observations. The correlation times extracted from the 2D exchange  $^2\text{H}$  NMR experiments agree well with values found by photon correlation spectroscopy (PCS);<sup>28</sup> vide infra. Therefore, on the time scale of the  $\alpha$ -relaxation the geometry of motion is best described as a planar diffusion, inferring the time scale of conformational transitions to be rather slow. Spectra with mixing times longer than 500 ms were not recorded, because of the effective loss of signal intensity due to  $T_1$  relaxation of the methylene groups, and furthermore, the onset of spin diffusion, becoming the dominant mechanism for long mixing times and causing exchange intensity without molecular reorientation involved.

Note that in 2D exchange  $^{13}\text{C}$  NMR spectra of the carboxyl side group in PEMA at a slightly higher temperature ( $T_g + 17$  K) about 15% of the carboxyl segments appear in their original position after 500 ms, presumably in contrast to the observation made here by applying 2D exchange  $^2\text{H}$  NMR, where all backbone segments are found to participate in the main chain reorientation. Apparently, the diagonal intensity of the  $^{13}\text{C}$  spectra is caused by carboxyl segments that are not rigid but whose chemical shift tensor components are

found parallel to their initial directions due to the superposition of the main chain rotation and the  $180^\circ$  flip of the side groups. Since in this temperature range the  $^{13}\text{C}$  spectra are sensitive to both the  $\alpha$ - and  $\beta$ -process with correlation times in the slow motion limit and intermediate regime, respectively, a separation and quantification of those two contributions with their different correlation times proves to be difficult. Therefore, the motional geometry of the  $\alpha$ -relaxation can only be unambiguously monitored at a moiety not sensitive to the carboxyl group flip itself, that is, deuterons in the main chain of PEMA.

At a higher temperature (365 K), it has been previously shown by 3D difference correlated (DICO) NMR<sup>8</sup> that the chain dynamics in PEMA consists of pronounced small-angle fluctuations and large-angle (jump-type) motions associated with conformational transitions. The occurrence of conformational transitions above the glass transition has been directly proven for a variety of amorphous polymers,<sup>29</sup> including PEMA, by utilizing the  $\gamma$ -gauche effect in high-resolution 2D exchange solid-state  $^{13}\text{C}$  NMR.

Albeit, the 2D exchange spectra of PEMA- $d_5$  at and above this temperature can also be fitted reasonably well by employing the model of isotropic rotational diffusion with a distribution of correlation times for the following reasons. Firstly, for jump-type motions without a well-defined jump angle being present on roughly the same time scale as small-angle diffusion, the spectral shape is completely dominated by the diffusive motion. Secondly, the distribution of correlation times effectively mimics the two different types of motion, namely the slowly diffusing segments representing the



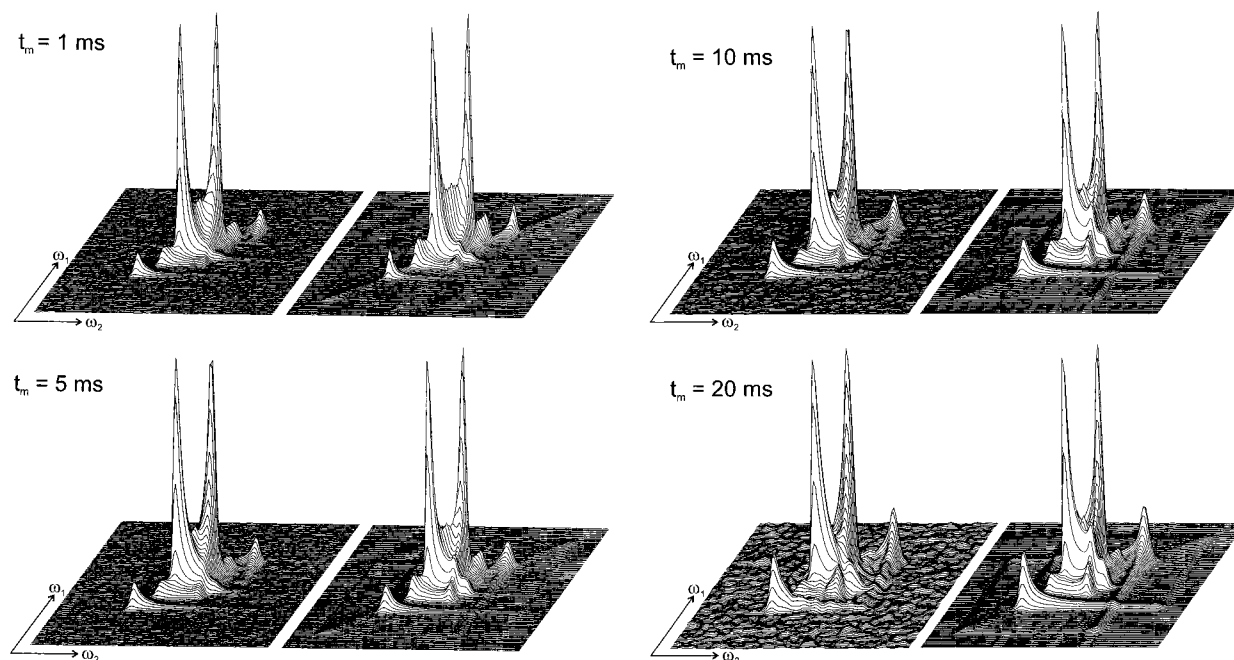


**Figure 7.** 2D exchange  $^2\text{H}$  NMR spectra (left columns, respectively) of PEMA- $d_5$  at 380 K ( $T_g + 35$  K) and the indicated mixing times, demonstrating a mobility on a millisecond time scale. The spectra show no characteristic exchange ridges, and since the small peak in the center of the spectrum indicates fast and isotropic reorienting segments, the corresponding simulations (right columns, respectively) were performed for isotropic rotational diffusion with a mean correlation time of  $\langle\tau_c\rangle = 1.5$  ms and a symmetric log-Gaussian distribution of 2.4 decades (fwhm), calculated according to eq 6.

small-angle motions, while the segments with a fast diffusion rate represent the jump-type motions. Therefore, in summary, isotropic rotational diffusion with a distribution of correlation times captures the essential features of the main chain dynamics and will be used to quantify the time scale of the motion in PEMA in the following. Considering the dynamics during all time periods of the exchange experiment, according to eq 6, to account for the relatively broad distribution of correlation times as well as the coupling of the main chain to the fast side group motion, the mean correlation time extracted from a series of 2D spectra was  $12 \pm 5$  ms with a symmetric log-Gaussian distribution with a  $2.4 \pm 0.3$  decade fwhm at 365 K.<sup>8</sup>

2D exchange  $^2\text{H}$  NMR spectra of PEMA- $d_5$  acquired at a higher temperature of 380 K (Figure 7, left columns, respectively) exhibit considerable exchange intensity, extending over the entire spectral plane already for mixing times of a few milliseconds, and hence can well be seen also in the spectra of the methyl deuterons, which have not yet significantly been reduced in intensity by longitudinal relaxation. The appearance of a small peak in the center of the broad powder spectrum, originating from segments whose quadrupolar interaction is isotropically averaged ( $\tau_c < 1 \mu\text{s}$ ), directly proves that the dynamic behavior is characterized by a heterogeneous distribution of correlation times and demonstrates the necessity to consider in simulations the dynamics not only during the mixing time but also during the whole course of the 2D experiment. Nevertheless, for a mixing time of 20 ms, each cross section of the 2D spectrum parallel to the frequency axes closely resembles a 1D powder pattern, indicating that the approximation of the slow motion limit is still not strongly violated and furthermore that the motion is indeed isotropic, since only in that case does the 2D spectrum consist essentially of the product of two 1D spectra.<sup>18</sup> The simulations (Figure 7, right columns, respectively) for the model of isotropic rotational diffusion based on  $\langle\tau_c\rangle = 1.5 \pm 1$  ms and  $2.4 \pm 0.3$  decades

fwhm agree well with the experimental spectra. Small deviations arise from anisotropic  $T_1$  and  $T_{1Q}$  relaxations and result in less intensity along the subdiagonal of the experimental line shapes, especially at the  $90^\circ$  ridges. Other slight differences in the diagonal intensity, being higher in the central part and lower at the edges, are due to the coupling to the fast  $\beta$ -process and finite pulse length effects, diminishing the intensity at the edges of the spectra.

Since an extraordinarily high conformational order of the local chain axis was found in the one-dimensional  $^{13}\text{C}$  NMR spectra of the carboxyl side group in PEMA at 395 K ( $T_g + 55$  K),<sup>5</sup> it is interesting to test whether evidence for this anisotropic rocking motion of the chain on the fast time scale of the  $\beta$ -process can be found also on a longer (millisecond) time scale probed by 2D exchange  $^2\text{H}$  NMR. 2D  $^2\text{H}$  NMR spectra for two different mixing times acquired at a temperature of 390 K ( $T_g + 45$  K) are shown in Figure 8. While the spectrum for  $t_m = 1$  ms already exhibits considerable exchange intensity, not all possible orientations are reached, as evident from the comparison with the 2D spectrum for 5 ms, which displays an even higher exchange intensity, the shape of which demonstrates that now all possible orientations have indeed been reached on the time scale of 5 ms. A comparison with the simulations in Figure 8 (right column) yields an average correlation time of  $\langle\tau_c\rangle = 0.2 \pm 0.1$  ms and a distribution of  $1.8 \pm 0.2$  decades fwhm. Therefore, the order parameters revealed by the 1D  $^{13}\text{C}$  NMR spectra are identified clearly as resulting from a transient phenomenon,<sup>5</sup> existing only for less than a few microseconds, but decreasing to zero on a millisecond time scale.

Whereas 2D exchange  $^2\text{H}$  NMR spectra are sensitive to both modes of motion, i.e., perpendicular to the chain axis and of the chain axis itself, 2D exchange  $^{13}\text{C}$  NMR spectra of the carboxyl carbon, preaveraged by the  $180^\circ$  flip in conjunction with a fast rocking motion around the local chain axis  $Z$  (the unique axis of the uniaxially

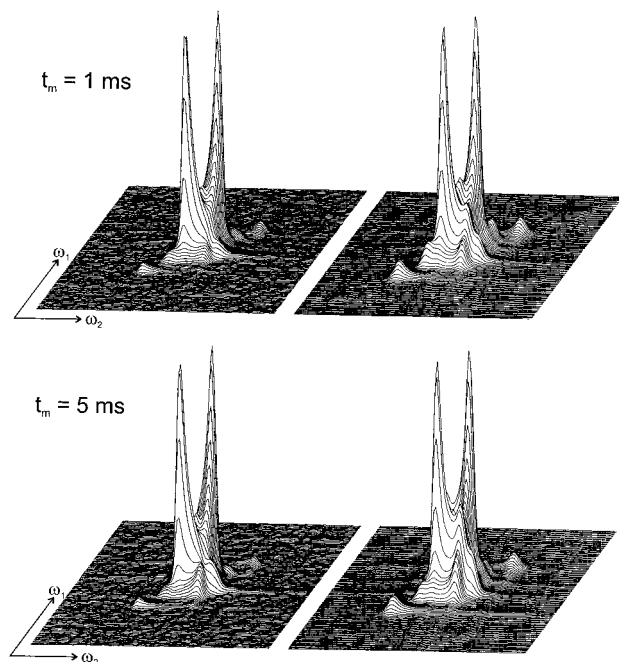


**Figure 8.** 2D exchange  $^2\text{H}$  NMR spectra (left column) of PEMA- $d_5$  at 390 K ( $T_g + 45$  K) and the indicated mixing times. As can be seen from the comparison of the intensity of the  $90^\circ$  exchange ridges with the diagonal intensity, isotropic reorientation of segments takes place within 5 ms, since each slice through the 2D spectrum exhibits the line shape of the 1D powder spectrum. The simulations (right column) for isotropic rotational diffusion calculated according to eq 6 yield an average correlation time of  $\langle\tau_c\rangle = 0.2$  ms and a distribution width of 1.8 decades (fwhm). On the time scale of the  $\beta$ -process (a few microseconds at this temperature), however, the chain motions are highly anisotropic, with the rotation around the chain axis being much faster than the reorientation of the chain axis itself.

averaged chemical shift tensor), are capable of selectively probing the reorientation of the chain axis itself, because the other mode, i.e., the slower planar rotation around the local chain axis ( $\alpha$ -process), does not lead to exchange intensity. Unfortunately, since the shortest possible mixing time is 1 ms and since complete isotropization of the chain motion is already reached after 5 ms, the reorientation of the chain axis itself is already too fast to be studied by 2D exchange  $^{13}\text{C}$  NMR to reveal any differences to the motion parallel and perpendicular to the local chain axis in PEMA. This observation is consistent with the findings of  $^2\text{H}$  and  $^{13}\text{C}$  NMR that also at lower temperatures near  $T_g$ , rotation around the local chain axis  $Z$ , that is, the dynamics perpendicular to  $Z$ , is much faster than the reorientation of the chain axis itself.

**Correlation Times of the  $\alpha$ - and  $\beta$ -Relaxations in PEMA.** The temperature dependence of the mean correlation times of the  $\alpha$ - and  $\beta$ -relaxations in PEMA, as revealed in the current investigation by 2D exchange  $^2\text{H}$  NMR (●) and one- and two-dimensional exchange  $^{13}\text{C}$  NMR<sup>3</sup> (□), respectively, is summarized in the Arrhenius-type diagram in Figure 9 and compared to the results from photon correlation spectroscopy<sup>28</sup> (▲) and dielectric relaxation measurements<sup>30</sup> (◇). Dielectric relaxation measurements detect the changes of the electric dipole moment caused by dynamics of the carboxyl side group and are therefore primarily sensitive to the  $\beta$ -relaxation, as is  $^{13}\text{C}$  NMR of the carboxyl carbon, evident by the good agreement of the correlation times obtained by both methods.

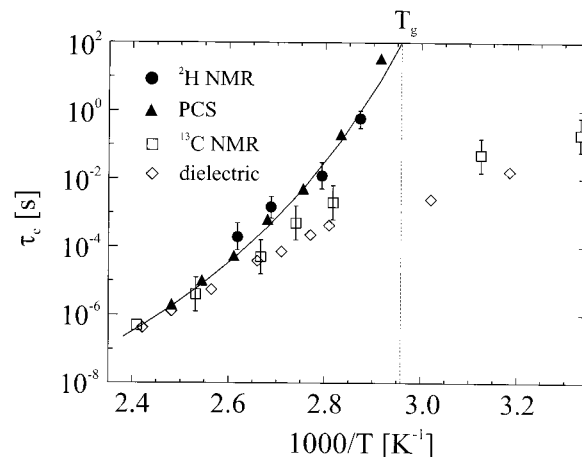


**Figure 9.** Mean correlation times versus temperature for the  $\alpha$ - and  $\beta$ -relaxations in PEMA. The correlation times of the  $\alpha$ -process obtained from the current 2D exchange  $^2\text{H}$  NMR investigation (●) agree well with those from photon correlation spectroscopy<sup>28</sup> (PCS) (▲). The correlation times of the  $\beta$ -process were determined by one- and two-dimensional  $^{13}\text{C}$  NMR<sup>3</sup> (□) and dielectric spectroscopy<sup>30</sup> (◇). All data were scaled to a common glass transition temperature  $T_g = 338$  K. The solid line represents a WLF curve with parameters of  $C_1 = 15.5$  and  $C_2 = 65$  K, with  $\tau_c(T_g)$  set to 100 s.

Light scattering is caused by fluctuations of the dielectric tensor, which are proportional to slowly relaxing density fluctuations and hence molecular motions in the sample. Accordingly, the decay of the density-density autocorrelation function measured by photon correlation spectroscopy (PCS) can be related to the  $\alpha$ -process in amorphous polymers and is often quantified by fitting to a stretched exponential  $\exp(-t/\tau_c)^{\beta_{\text{KWW}}}$  (Kohlrausch-Williams-Watts, KWW) function. PCS studies of PEMA revealed a nonlinear temperature dependence of the mean correlation times typical for amorphous polymers above the glass transition, accompanied by a considerable increase in the width of the distribution of correlation times, ranging from a distribution characterized by a parameter  $\beta_{\text{KWW}} = 0.4$  at 393 K to a value of less than 0.2 when approaching  $T_g$  from higher temperatures. The variable distribution width was attributed to the presence of two different relaxation processes, i.e.,  $\alpha$ - and  $\beta$ -relaxations, with different temperature dependencies of the correlation times, eventually merging at high temperatures. As the mean correlation time obtained from PCS measurements is dominated by the slow portion of the relaxation time distribution,<sup>28</sup> the correlation times were concluded to be mainly sensitive to the  $\alpha$ -relaxation. This assumption is corroborated by the agreement of the correlation times obtained by PCS and  $^2\text{H}$  NMR spectroscopy as compared to the correlation times of the  $\beta$ -process revealed by  $^{13}\text{C}$  NMR and dielectric measurements. Applying high pressure, the  $\alpha$ - and  $\beta$ -processes could be separated in a later PCS study,<sup>31</sup> with the  $\alpha$ -process showing an almost temperature independent distribution parameter  $\beta_{\text{KWW}} = 0.35$ , equivalent to a distribution approximately 3 decades wide (fwhm).<sup>32</sup> Similar observations have been made in 2D exchange  $^2\text{H}$  NMR: Within a temperature interval from 365 to 390 K, the distribution width is slightly reduced from 2.4 to 1.8 decades, while the width parameters are generally found to be smaller than the values found by PCS. The differences probably result from the different distribution functions used: The 2D exchange spectra are somewhat insensitive to the exact shape of the correlation time distribution, and therefore, for the sake

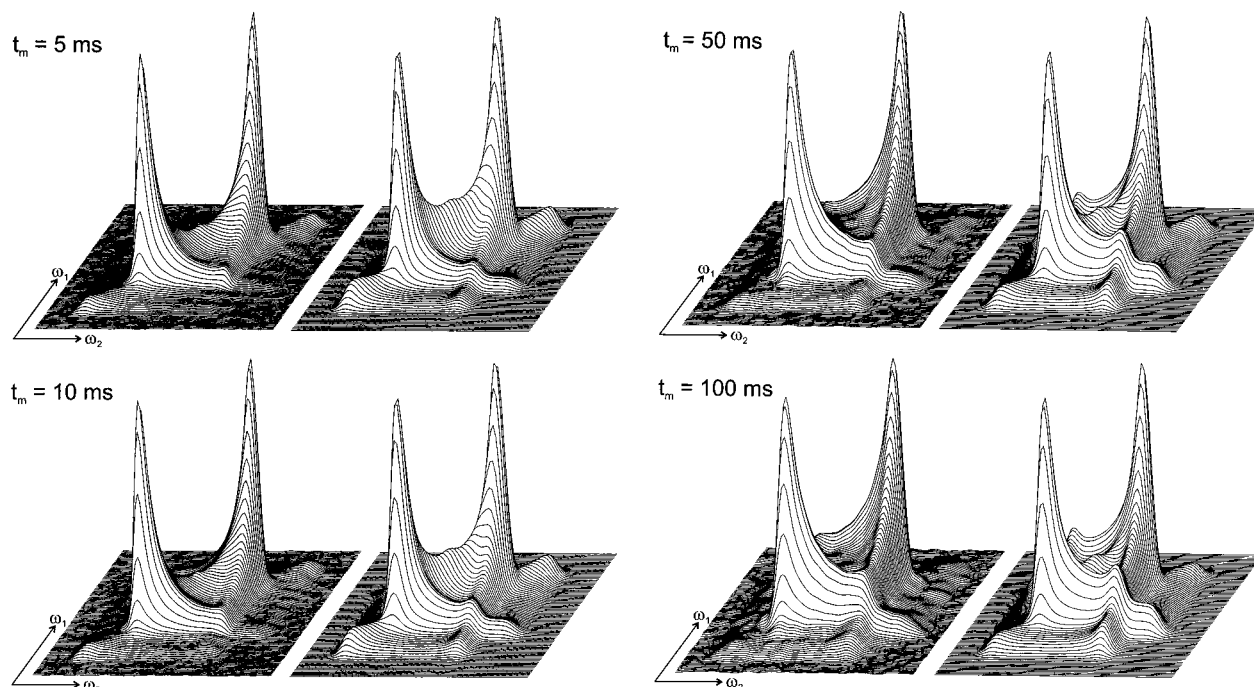


**Figure 10.** 2D exchange  $^2\text{H}$  NMR spectra (left columns, respectively) of PMMA- $d_3$  at 405 K ( $T_g + 10$  K), used as a probe for main chain reorientations. To account for the diffusive appearance of the exchange intensity and the small isotropic peak in the center of the spectra, simulations for isotropic rotational diffusion (right columns, respectively) were performed according to eq 6, yielding a mean correlation time of  $\langle\tau_c\rangle = 6$  ms and a Gaussian distribution width of 2.7 decades (fwhm). The spectra demonstrate that already at temperatures near  $T_g$  the main chain in PMMA is highly mobile and reorients isotropically, contrary to PEMA- $d_5$ , where the backbone dynamics is slower by 2 orders of magnitude and anisotropic.

of simplicity, generally a symmetric log-Gaussian distribution is used in the analysis. The insensitivity to a particular shape is especially pronounced for intermediate correlation times on the order of a few microseconds to several hundred microseconds because of the generally drastically reduced NMR signal intensity in this intermediate correlation time regime. This results in an underestimate of the width parameter, unless a significant amount of molecules is reorienting on an even faster time scale, contributing a narrow averaged peak to the exchange NMR spectrum, which is, however, not the case for the materials investigated here. In contrast, the distribution function corresponding to a KWW function is asymmetric, with a long tail toward small correlation times, and thus larger values for the distribution width parameters commonly result.

Likewise, recent dielectric measurements of the relaxation processes in poly(*n*-alkyl methacrylates)<sup>10</sup> revealed two relaxation processes in PEMA below a temperature of 370 K, with the slow and fast relaxation mode attributed to the  $\alpha$ - and  $\beta$ -processes, respectively. The dielectrically measured correlation times for the  $\alpha$ -relaxation agree quite well with the present 2D  $^2\text{H}$  NMR data. Similarly, a splitting of the  $\alpha$ - and  $\beta$ -processes around  $T_g$  has been observed also by mechanical spectroscopy.<sup>33</sup>

The temperature dependence of the mean correlation times of  $^2\text{H}$  NMR and PCS can be characterized by fitting the Williams–Landel–Ferry (WLF) equation<sup>34</sup>

$$\log a_T = \log \frac{\tau_c(T)}{\tau_c(T_g)} = - \frac{C_1(T - T_g)}{C_2 + (T - T_g)} \quad (7)$$

The fit is represented by the solid line in Figure 9, with parameters of  $C_1 = 15.5$  and  $C_2 = 65$  K; the correlation time at the glass transition temperature  $\tau_c(T_g)$  was set to 100 s and the glass transition temperatures of the

different samples were scaled to a common glass transition temperature of  $T_g = 338$  K. Similar values of  $C_1 = 17.6$  and  $C_2 = 65.5$  K with  $T_g = 335$  K and a shift parameter  $a_T = 3.7 \times 10^{-4}$  were obtained earlier from dynamic-mechanical measurements on a PEMA sample with an average molecular weight  $M_w \approx 1.6 \times 10^5$  g/mol.<sup>35</sup>

**2D Spectra of PMMA.** 2D exchange  $^2\text{H}$  NMR spectra of PMMA- $d_5$  reported recently<sup>24</sup> indicated a particularly high mobility above  $T_g$  with a mean correlation time  $\langle\tau_c\rangle = 3$  ms (with uncertainty limits of 1 ms and 6 ms) and a symmetric log-Gaussian distribution width of  $3 \pm 0.3$  decades fwhm at 407 K ( $T_g + 9$  K), and  $\langle\tau_c\rangle = 0.15$  ms (uncertainty limits of 0.1 and 0.3 ms) and  $2.3 \pm 0.3$  decades fwhm at 413 K,  $\tau_c$  values that are distinctly faster than observed in PEMA. However, due to the short relaxation times of the methyl group, spectra could not be recorded for mixing times much longer than 20 ms. Since the  $T_1$  relaxation time of the deuterated methoxy group, which can be used as a probe for main chain reorientation as explained above, is considerably longer ( $\approx 1$  s), 2D exchange  $^2\text{H}$  NMR spectra for PMMA- $d_3$  were recorded to check the results obtained for PMMA- $d_5$ .<sup>24</sup> A series of spectra with different mixing times acquired at a temperature of 405 K ( $T_g + 10$  K) is shown in Figure 10 (left columns, respectively). Significant exchange intensity is observed already for  $t_m = 5$  ms, and a small isotropic peak is visible in the center. The line shapes indicate that after a time of 100 ms all orientations in the powder sample have been reached. By comparison with simulations for isotropic rotational diffusion in Figure 10 (right columns, respectively), an average correlation time of  $\langle\tau_c\rangle = 6 \pm 3$  ms and a distribution width of  $2.7 \pm 0.3$  decades fwhm is extracted. As observed also for PEMA- $d_5$ , the diagonal intensity in the experimental spectra is smaller than in the simulations for short mixing times, indicat-

ing an asymmetric distribution of correlation times caused by fast moving segments on the time scale of the  $\beta$ -process. In summary, the almost identical line shapes and simulation parameters of the 2D spectra of PMMA- $d_3$  and those of main chain deuterated PMMA- $d_5$  at the respective temperatures demonstrate the high mobility of PMMA above the glass transition, not only relative to other methacrylate polymers, but also to, for example, polystyrene, which has a glass transition temperature similar to that of PMMA. While in PS ( $T_g = 373$  K), the mean correlation time is 12 ms at  $T^* = T/T_g = 1.05$ , it is smaller by 2 orders of magnitude (0.15 ms) in PMMA at  $T^* = 1.05$ ; additionally, the distribution of correlation times in PS of ca. 3.5 decades (fwhm) is wider by about one decade. These differences are even more pronounced when compared to atactic polypropylene ( $T_g = 253$  K), where the average correlation time is  $\langle\tau_c\rangle = 320$  ms with fwhm 2.5 decades at a reduced temperature of  $T^* = 1.04$ , the chain dynamics thus being slower by 3 orders of magnitude than in PMMA.

Slightly longer correlation times for the  $\alpha$ -relaxation in PMMA are observed by photon correlation spectroscopy<sup>36</sup> with correlation times of  $\langle\tau_c\rangle = 2.5$  ms at 407 K, 19 K above  $T_g$ , determined as 388 K from the temperature at which  $\langle\tau_c\rangle \cong 100$  s, with a distribution parameter  $\beta_{KWW} = 0.23$ , and  $\langle\tau_c\rangle = 0.7$  ms with  $\beta_{KWW} = 0.26$  at 413 K. The large distribution width indicates the existence of two different relaxation processes analogous to PEMA, which was confirmed in a later PCS study.<sup>37</sup> Similar results are obtained from dielectric spectroscopy,<sup>10</sup> where the data were fitted by two Havriliak–Negami functions to account for the simultaneous presence of  $\alpha$ - and  $\beta$ -processes above the glass transition; in this investigation, the average correlation time for the  $\alpha$ -process was reported to be a few milliseconds at 20 K above  $T_g$ .

## V. Summary

The dynamics in amorphous PMMA and PEMA has been investigated in detail by 2D exchange NMR below and above the glass transition temperature and the influence of structural variations on the microscopic dynamics of the backbone motions has been elucidated. Below the glass transition temperature, the proposed coupling of the  $\beta$ -process, essentially comprising a 180° flip of the carboxyl side group, to a restricted rotation of the main chain in a static molecular potential has been confirmed and was analyzed quantitatively, with PEMA exhibiting a slightly larger rotation amplitude and a higher fraction of mobile segments near  $T_g$  than PMMA.

Both polymers behave differently at and above  $T_g$ : In PMMA, the rocking motion of the polymer backbone already present in the glassy state evokes a pronouncedly higher mobility of the main chain above the glass transition when compared to higher poly( $n$ -alkyl methacrylates) and also to other amorphous polymers like polystyrene or atactic polypropylene. Therefore, the coupling of the main chain motions to the  $\beta$ -process influences the time scale of the  $\alpha$ -relaxation itself, leading to smaller correlation times. In contrast, a slow uniaxial rotation around the local chain axis sets in for PEMA at the glass transition, and consequently, the coupling of side group and main chain motions has its main impact on the geometry of main chain motions. The dissimilar behavior of both polymers can be explained by the correlation times of the  $\beta$ -process being slower by 1 order of magnitude at  $T_g$  in PEMA, and,

moreover, by the carboxyl side group motion retaining its anisotropic character above the glass transition. In PEMA, the larger ester side group induces an anisotropy of the main chain motions, bringing about differences in the correlation times perpendicular and parallel to the local chain axis, and resulting in longer mean correlation times. This behavior is observed not only at  $T_g$ , but also at higher temperatures ( $\sim T_g + 45$  K): though the main chain motions lead to an isotropic reorientation on a time scale of a few milliseconds, the side group motions show a fast anisotropic averaging in 1D  $^{13}\text{C}$  NMR spectra. In contrast, the small and highly mobile side group in PMMA can only couple to the time scale of the  $\alpha$ -process dynamics, inferring a particularly high mobility of the backbone motion itself. The agreement of the correlation times found by 2D exchange NMR and photon correlation spectroscopy corroborates the ability of the microscopic probe in  $^2\text{H}$  NMR to pursue the cooperative dynamics of the  $\alpha$ -process.

**Acknowledgment.** Financial support from the Deutsche Forschungsgemeinschaft (SFB 262) is gratefully acknowledged. A donation from the Dr. Röhm Gedächtnisstiftung is highly appreciated.

## References and Notes

- (1) Ferry J. D. *Viscoelastic Properties of Polymers*, 3rd ed.; Wiley: New York, 1980.
- (2) Schmidt-Rohr, K.; Kulik, A. S.; Beckham, H. W.; Ohlemacher, A.; Pawelzik, U.; Boeffel, C.; Spiess, H. W. *Macromolecules* **1994**, *27*, 4733.
- (3) Kulik, A. S.; Beckham, H. W.; Schmidt-Rohr, K.; Radloff, D.; Pawelzik, U.; Boeffel, C.; Spiess, H. W. *Macromolecules* **1994**, *27*, 4746.
- (4) Schmidt-Rohr, K.; Spiess, H. W. *Multidimensional Solid State NMR and Polymers*; Academic Press: London, New York, 1994.
- (5) Kulik, A. S.; Radloff, D.; Spiess, H. W. *Macromolecules* **1994**, *27*, 3111.
- (6) Demco, D. E.; Hafner, S.; Fülber, C.; Graf, R.; Spiess, H. W. *J. Chem. Phys.* **1996**, *105*, 11285.
- (7) Pschorn, U.; Rössler, E.; Sillescu, H.; Kaufmann, S.; Schaefer, D.; Spiess, H. W. *Macromolecules* **1991**, *24*, 398.
- (8) Kuebler, S. C.; Heuer, A.; Spiess, H. W. *Macromolecules* **1996**, *29*, 7089.
- (9) Heuer, A.; Leisen, J.; Kuebler, S. C.; Spiess, H. W. *J. Chem. Phys.* **1996**, *105*, 7088.
- (10) Garwe, F.; Schönhals, A.; Lockwenz, H.; Beiner, M.; Schröter, K.; Donth, E. *Macromolecules* **1996**, *29*, 247.
- (11) McCrum, N. G.; Read, B. E.; Williams, G. *Inelastic and Dielectric Effects in Polymeric Solids*; Wiley: New York, 1991.
- (12) Beiner, M.; Garwe, F.; Schröter, K.; Donth, E. *Colloid. Polym. Sci.* **1994**, *272*, 1439.
- (13) Schmidt, C.; Blümich, B.; Spiess, H. W. *J. Magn. Reson.* **1988**, *79*, 390.
- (14) Schaefer, D.; Leisen, J.; Spiess, H. W. *J. Magn. Reson. A* **1995**, *115*, 60.
- (15) Wefing, S.; Kaufmann, S.; Spiess, H. W. *J. Chem. Phys.* **1989**, *89*, 1234.
- (16) Schaefer, D.; Spiess, H. W.; Suter, U. W.; Fleming, W. W. *Macromolecules* **1990**, *23*, 3431.
- (17) Schaefer, D.; Spiess, H. W. *J. Chem. Phys.* **1992**, *97*, 7944.
- (18) Kaufmann, S.; Wefing, S.; Schaefer, D.; Spiess, H. W. *J. Chem. Phys.* **1990**, *93*, 197.
- (19) Spiess, H. W.; Sillescu, H. *J. Magn. Reson.* **1981**, *42*, 381.
- (20) Schilling, F. C.; Bovey, F. A.; Bruch, M. D.; Kozolowski, S. A. *Macromolecules* **1985**, *18*, 1418.
- (21) Goni, I.; Gurruchaga, M.; Valero, M.; Guzman, G. M. *Polymer* **1992**, *33*, 3089. Gurruchaga, M.; Goni, I.; Vazquez, B.; Valero, M.; Guzman, G. M. *Macromolecules* **1992**, *25*, 3009.
- (22) Lovell, R.; Windle, A. H. *Polymer* **1981**, *22*, 175.
- (23) Vacatello, M.; Flory, P. J. *Macromolecules* **1986**, *19*, 405. Vacatello, M.; Yoon, D. Y.; Flory, P. J. *Macromolecules* **1990**, *23*, 1993.
- (24) Kuebler, S. C.; Schaefer, D. J.; Boeffel, C.; Pawelzik, U.; Spiess, H. W. *Polym. Prepr. (Am. Chem. Soc., Div. Polym. Chem.)* **1997**, *38* (1), 821.

- (25) Domberger, W.; Reichert, D.; Garwe, F.; Schneider, H.; Donth, E. *J. Phys.: Condens. Matter* **1995**, *38*, 7419.
- (26) Vega, A. J. *Polym. Prepr. (Am. Chem. Soc., Div. Polym. Chem.)* **1981**, *22*, 282.
- (27) Dabbagh, G.; Weliky, D. P.; Tycko, R. *Macromolecules* **1994**, *17*, 6183.
- (28) Patterson, G. D.; Stevens, J. R.; Lindsey, C. P. *J. Macromol. Sci., Phys.* **1980**, *18*, 641.
- (29) Zemke, K.; Chmelka, B. F.; Schmidt-Rohr, K.; Spiess, H. W. *Macromolecules* **1991**, *24*, 6874. Zemke, K. Ph.D. Thesis, Mainz, 1994.
- (30) Ishida, Y.; Yamafuji, K. *Kolloid-Z.* **1961**, *177*, 97.
- (31) Fytas, G.; Patkowski, A.; Meier, G.; Dorfmueller, Th. *Polymer* **1983**, *24*, 2214.
- (32) Fytas, G.; Meier, G.; Dorfmueller, Th.; Patkowski, A. *Macromolecules* **1982**, *15*, 214.
- (33) Beiner, M.; Garwe, F.; Schroter, K.; Donth, E. *Polymer* **1994**, *35*, 4127.
- (34) Williams, M. L.; Landel, R. F.; Ferry, J. D. *J. Am. Chem. Soc.* **1955**, *77*, 3701.
- (35) Ferry, J. D.; Child, W. C., Jr.; Zand, R.; Stern, D. M.; Williams, M. L.; Landel, R. F. *J. Colloid. Sci.* **1957**, *12*, 53.
- (36) Patterson, G. D.; Carroll, P. J.; Stevens, J. R. *J. Polym. Sci., Polym. Phys. Ed.* **1983**, *21*, 613.
- (37) Fytas, G.; Wang, C. H.; Fischer, E. W.; Mehler, K. *J. Polym. Sci., Polym. Phys. Ed.* **1986**, *24*, 1859.

MA9708757